Food Science and Engineering
http://ojs.wiserpub.com/index.php/FSE/

Research Article

Changes in Moisture Desorption Rate of Shelled Corn Layers in a Low-Temperature Deep-Bed Drying Column

Xingjun Li[1*], Huan Zhang[2], Zidan Wu[1,2], Wenfu Wu[2]

[1]National Engineering Research Center for Grain Storage and Transportation, Academy of National Food and Strategic Reserves Administration, Beijing, China
[2]College of Biological and Agricultural Engineering, Jilin University, Changchun, China
E-mail: lxj@ags.ac.cn

Received: 18 September 2023; **Revised:** 31 January 2024; **Accepted:** 23 February 2024

Abstract: To optimize grain drying processes, high-moisture shelled corn was dried in a device using a combination of three temperatures (45, 55 and 65 °C) and hot-air velocities (0.7, 1.1 and 1.3 $m \cdot s^{-1}$). The grain moisture and temperature, and the relative humidity (RH) of interstitial airflow were determined intelligently in grain layers of 7.5 to 32.5 cm with 5.0 cm intervals. The change in RH of interstitial airflow in grain layers of 7.5-27.5 cm with drying time all revealed the shape of a hyperbolic line and took turns to lag. These RH lines shortened with an increased drying temperature from 45 to 65 °C and hot-air velocity from 0.7 to 1.3 $m \cdot s^{-1}$. The temperature lines were raised and shortened with an increase in drying temperature and hot-air velocity. A modified moisture diffusion exponential equation was developed to analyze the moisture desorption rate of corn kernels. For the average sorption rate curve from grain layers of 2.5-32.5 cm at 1.3 $m \cdot s^{-1}$ of hot air, the transition points from adsorption to desorption occurred at 2.4 h, 2.7 h, and 3.0 h with drying temperatures of 65 and 45 °C, respectively, and represented the earliest and largest initial desorption rates among the three hot-air velocities. The moisture desorption rate of samples increased with increasing drying temperature. Compared with the average value of grain layers, at the same hot-air velocity, the kernel effective diffusivity (D_{eff}) values dried at 55 °C were correspondingly higher than those dried at 45 and 65 °C. At the same drying temperature, the kernel D_{eff} values tended to increase with an increase in hot-air velocity, whereas the activation energy decreased. These results suggested that an increase in drying temperature and hot-air velocity may considerably shorten adsorption time and increase desorption rates of shelled corn in deep bed drying.

***Keywords*:** shelled corn, moisture desorption rate, diffusion equation, deep-bed drying column, slab shape, smart detection

1. Introduction

Corn is one of the main grain crops in China and its production in North China accounts for 20-27% of the annual grain yield. Corn is a late-autumn crop, and the local weather is often poor during the harvest period, which leads to a high moisture content (MC) of harvested corn. In the northeast region of China, the majority of acquired shelled corn has a high MC of 20-25% wet basis (w.b.) on average, reaching >35% in individual years [1]. Following harvest, shelled corn is dried to <14% w.b. MC for long-term storage [2]. In currently used corn dyers in China, the regulation of

DOI: https://doi.org/10.37256/fse.5120243683

the drying process is not accurate, the moisture distribution in grain kernels following drying is uneven, corn quality is decreased following drying, and power consumption is higher. Since the amount of corn that must be dried per unit time is increasing due to increased production demands, harvesting, and transportation capabilities, it is imperative to study the basis and process of drying high-moisture corn in order to improve the dryer throughout rates in the main maize growing regions of China.

Grain drying is required when the MC of grain poses a threat to safe storage and transportation and is an inevitable component of grain processing, which includes production, storage, and utilization [3]. During grain drying, moisture is transferred from a whole grain to the air and the latent heat required to vaporize the moisture is supplied by the drying air [4]. Thus, drying is a simultaneous process of heat and mass transfer [5-6]. It is important to understand the changes in the grain temperature and MC and to clarify the effects of drying conditions during the grain drying process, as this may be useful in improving the efficient use of current grain dryers and developing new grain dryers; therefore, mathematical modeling is very important.

There are numerous available food drying mathematical models such as the Page equation, the Newton model, the Wang and Singh model, and so on [5, 7]. A number of empirical equations developed have as good, or greater, accuracy in a specific application with less computational effort compared with theoretical equations [8-9]. The exponential drying equation has been useful in certain cases for describing thin-layer drying though it provides a poor description of the initial part of the drying process [10]. Page developed an empirical equation that has proven to be more accurate compared with the exponential drying equation [11]. Following numerous years of widespread use, the Page equation is now accepted as the preferred equation for drying work [12]. The moisture desorption from grain kernels during drying nearly always occurs in the falling-rate drying period, in which there is no free moisture. The resulting two coupled partial differential equations describing heat and moisture diffusion may be uncoupled due to the different rates of heat transfer, as compared with mass transfer during drying [13]; therefore, thin-layer drying equations are referred to herein as diffusion equations. The diffusion equations are usually based on the assumption that grain kernels are homogeneous. Walton and Casada [14] developed cellular diffusion-based equations based on the actual non-homogeneous internal cell structure of foliar material. These models account for various resistances to moisture diffusion within the biological material by allowing finite resistance to moisture at the surface. A specific cellular diffusion based drying model was applied to a wide range of drying data for shelled corn by Walton et al. [15] and was revealed to fit the data more closely compared with the Page equation. A literature review demonstrated no sufficient data for modeling moisture desorption rates of shelled corn with an increase in grain bed depth [16-17].

An equation describing the thin-layer drying rate is required for the simulation of deep bed drying, since simulation models are usually based on the assumption that the deep bed is composed of a number of thin-layers of product [18]. Previous studies [1, 19] revealed that the parameters k and n in thin-layer drying equations are not fixed, and their values depend largely on the experimental conditions and may not be appropriate for the drying of Chinese shelled corn.

The present study performed quantification of moisture desorption patterns of Chinese shelled corn within an experimentally simulated, low-temperature deep-bed drying column device. The objectives were to (i) quantify the effects of drying temperature and hot-air velocity treatments on moisture contents (MCs) and the moisture sorption rates as a function of drying time and location within the grain column; (ii) analyze the alterations in temperature and RH within the grain column, in particular by deep bed simulation, and determine the moisture transfer and equilibrium characteristics of shelled corn in the lower drying temperature range, with the aim of improving our understanding of the basic factors controlling the transfer of heat and mass within corn kernels, and provide a basis for the design and optimization of the corn drying processes, particularly the simulation of in-store drying systems.

2. Materials and methods

2.1 *Low-temperature deep-bed drying column apparatus*

The drying device comprised a fan, air pipe, electrical heater section, plenum, a set of seven sieves, temperature/humidity sensors, a computer, and a controlling cabinet, and supplied by Jida Scientific Instrument Co., LTD., Changchun, China (Figure 1). The low-noise centrifugal fan has power of 200 W, a frequency of 50 Hz, a full pressure of 660 Pa, and air volume of 604 $m^3 \cdot min^{-1}$. The thermostatic electrical heater adopts resistance wire with external

ceramic insulation and is 220 V and 40-50 W, producing a temperature range from room temperature to 80 °C and an accuracy of ±1 °C. The universal frequency converter (EDS1000) has a rated capacity of 1.1 kilovolt-ampere, and a rated output current of 3A. From the bottom to the top, the weight of a set of seven round-bottom aluminum sieves with 1.4-mm pore size was 304, 276, 296, 295, 297, 296, and 285 grams, respectively. The base sieve was 25 cm in diameter and 5 cm in depth, and this set of seven sieves was placed into high-moisture corn and assembled in sequence with a height of 35 cm. Among nine adopted digital temperature and relative humidity sensors (SHT 11), seven sensors were used for grain intergranular air, one sensor for exhaust air and one sensor for ambient air. The humidity sensor, SHT 11, has an accuracy of ±3% RH, and the temperature sensor with an accuracy of (0.15 + 0.002 × |T| °C). The air velocity was determined at the air exit using a handheld hot ball electric anemometer with a measuring range of 0.05-5 m/s and a resolution ratio of 0.01 m/s (QDF-2A, Zhongxi Yuanda Scientific Co., LTD., Beijing, China).

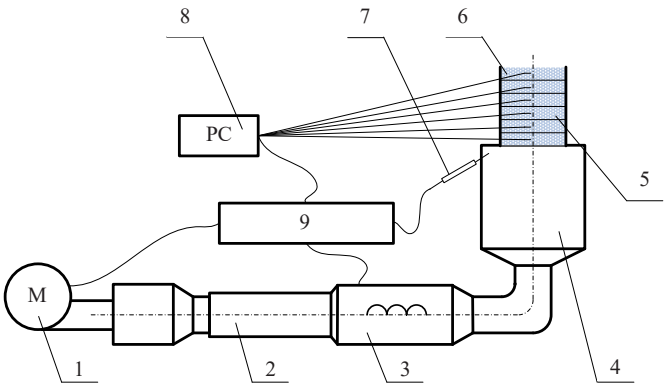

1. Fan; 2. Pipe; 3. Electrical heater section; 4. Plenum; 5. Deep-bed drying column;
6. Temperature and humidity sensor; 7. Temperature sensor; 8. Computer;
9. Controlling cabinet

Figure 1. Schematic diagram of the drying system

2.2 *Sample preparation*

A 50 kg bulk lot of shelled corn was collected from a farmer on 2 November 2014 with an initial *ca*. 26% MC, and immediately used for a drying experiment. All MCs were reported on a wet basis (w.b.) in the present study. The lot was cleaned by hand to remove foreign material and broken kernels. The 2 kg sub-lots were stored in sealed plastic bags at 4 °C for one week. The high MC of shelled corn was determined to be 25.5% using a two-step method according to China's national standard GB/T 5497-85 [20]. Firstly, the duplicate 20.00 g samples were dried using an intelligent drying oven (DHG9240A; ±0.5 °C; Blue Sky Test Instrument Co., Hangzhou, China) maintained at 105 °C for 40 min. Subsequently, the shelled corn was removed and ground coarsely prior to weighing 3.0000 g crude meal samples in duplicate and drying them in the oven at 105 °C for 3 h.

2.3 *Sample drying test*

High-moisture shelled corn samples were successively placed in each of the seven round-bottom sieves and dried in the deep-bed drying column apparatus (Figure 1). Approximately 1.65 kg corn sample was put into each sieve. The electrical weighing sensor (YZC-1B, rated load of 30 kg, safe overload of 150% F.S. and an accuracy of 1 g, Tailong Electronic Weighing Instrument Co., LTD, Shanghai, China), with an accuracy of 0.01 g of sample mass in each sieve, sensed the weight of the corn samples once every 30 min during drying and transferred the signal to the personal computer using the RS232 interface. The temperature in each sieve sample was recorded once every 20 sec by a temperature sensor and collected using LabVIEW software (Version 8.5, National Instruments, USA). From the bottom to the top of the drying sample column, at the successive depth of the corn bed (2.5, 7.5, 12.5, 17.5, 22.5, 27.5,

and 32.5 cm), the temperatures and RHs of airflow were evaluated once every 30 min during drying by temperature and RH sensor. The temperature and RH of exhaust air was also determined. The present study analyzed the treatment combinations of 45, 55, and 65 °C hot air with 0.7, 1.1, and 1.3 $m \cdot s^{-1}$ velocity, respectively. The drying experiments were performed twice. The change curves of grain temperature, RH and moisture ratio were made by Kaleidagraph for Windows version 4.54 software [21].

2.4 *Analysis of desorption rate*

The diffusion equation is considered in this study on the basis of an assumption that corn kernels are homogenous. In the analysis of grain drying, the coupling effect of grain temperature and moisture is considered for an accurate engineering design, but at a kernel scale, the grain temperature gradient during drying can be ignored [13]. When diffusion in a shelled corn kernel occurs at a given temperature, the moisture diffusion equation alone is sufficient for the determination of the moisture movement.

Page [11] revised the exponential equation (eq. (1)) through adding an exponent to the time variable in order to improve the fit result of the corn-drying data, and developed eq. (2).

$$MR = \exp(-kt) \tag{1}$$

$$MR = \exp(-kt^n) \tag{2}$$

Where MR is the average moisture ratio of corn grains at any given time, decimal; $MR = (M_t - M_e)/(M_0 - M_e)$; M_t is average moisture of the corn grains at any given time (t), decimal wet basis; M_e is the equilibrium moisture content (decimal wet basis); M_0 is initial moisture content at $t = 0$ (decimal wet basis); t is time from the onset of drying process (min); and k and n are specific constants. We give a modified form of Page's equation as below:

$$MR = a \exp\left[-kt^n \cdot \exp(-b/(\theta + 273))\right] \tag{3}$$

Where θ is the temperature (°C) and a, b, and n are equation parameters. k is drying constant (h^{-1}).

From eq. (3),

$$\mathrm{d}(M_t)/\mathrm{d}t = (M_0 - M_e) \cdot a \cdot \exp(-kt^n \exp(-b/(\theta + 273))) \cdot (-knt^{n-1} \exp(-b/(\theta + 273))) \tag{4}$$

Where $\mathrm{d}(M_t)/\mathrm{d}t$ is the moisture desorption rate of shelled corn kernels ($10^{-2} \cdot h^{-1}$).

Alterations in the average moisture ratio of corn kernels with time at various drying temperatures (45-65 °C) were fitted to eq. (3) for samples with various initial moisture contents (IMCs) using the non-linear regression procedure in SPSS version 17.0 for Windows (SPSS Inc., [22]), which minimizes the square sum of deviations between experimental and predicted data in a series of iterative steps, and the relative reduction between successive residual sums of squares is at most 1E-08. The quality of the fit of eq. (3) was evaluated using determination coefficient (R^2), residue sum of squares (RSS), standard error (SE), and mean relative percentage error (MRE). R^2 was a basic criterion for the selection of the most effective equation to fit the experimental data. In addition to R^2, the other statistical parameters, MRE as a percentage, RSS, and SE were used to determine the goodness-of-fit. Equations (5)-(8) were used for calculating R^2, RSS, SE, and MRE, respectively.

$$RSS = \sum_{i=1}^{n} (m_i - m_{pi})^2 \tag{5}$$

$$SE = \sqrt{\sum_{i=1}^{n} (m_i - m_{pi})^2 / (n-1)} \tag{6}$$

$$R^2 = 1 - \sum_{i=1}^{n}(m_i - m_{pi})^2 \Big/ \sum_{i=1}^{n}(m_i - m_{mi})^2 \tag{7}$$

$$MRE\% = 100\left|(m_i - m_{pi})/m_i\right|/n \tag{8}$$

Where m_i is an experimental value, m_{pi} is the predicated value, m_{mi} is the average of experimental values, and n is the number of observations. The quality of the fit of an equation was suitable for practical purposes when *MRE* was <10% [23].

2.5 *Effective moisture diffusivity and activation energy of shelled corn kernels during drying*

Moisture flow within a grain kernel occurs through diffusion in a liquid and/or vapor state [13]. Fick's second law of diffusion is used for explaining the falling rate period of the drying process [24]. The drying curves for moisture ratio vs. drying time for thin layer drying at different drying air temperatures were plotted and the effective moisture diffusivity was calculated from these curves. The present study assumed the geometry of shelled corn as a homogenous slab. The governing equation for axi-symmetric mass transfer in this case was as follows:

$$\frac{\partial M}{\partial t} = \frac{\partial}{\partial x}\left[\mathrm{D}_{eff}\frac{\partial M}{\partial x}\right] \tag{9}$$

Where M is the moisture concentration (decimal wet basis); t is the time variable (h); D_{eff} is the effective moisture diffusivity ($m^2 \cdot h^{-1}$); x is the coordinate of moisture diffusion along half the thickness (L) of the slab (mm). In applying eq. (9) to a corn kernel, the following assumptions were made:

$$\text{At } t = 0, -L \le x \le +L, M(x,0) = M_0;$$

$$\text{At } t > 0, x = \pm L, M(x,t) = M_e;$$

$$\text{At } t > 0, x = 0, \frac{\partial M}{\partial t} = 0.$$

The analytical solution of eq. (9) for the average moisture inside a single corn kernel is presented in eq. (10):

$$MR = \left(\frac{8}{\pi^2}\right)\sum_{n=0}^{\infty}\frac{1}{(2n+1)^2}\exp\left[-\frac{\pi^2(2n+1)^2}{4L^2}\mathrm{D}_{eff}t\right] \tag{10}$$

Where *MR* is the moisture ratio and L is the half thickness of the slab (mm). If only n = (0, 2) were considered, the expansion of eq. (10) can be presented as follows:

$$MR = 0.8106\exp\left(-\frac{2.4674\mathrm{D}_{eff}}{L^2}t\right) + 0.09006\exp\left(-\frac{22.2066\mathrm{D}_{eff}}{L^2}t\right)$$

$$+0.03242\exp\left(-\frac{61.685\mathrm{D}_{eff}}{L^2}t\right) \tag{11}$$

The first term of the series solution in eq. (11) would dominate the others. As a result, the natural logarithmic form

of eq. (11) is presented in eq. (12):

$$\ln(MR) = \ln(0.8106) - \left(\frac{2.4674}{L^2}\right) D_{eff} t \tag{12}$$

Effective moisture diffusivity was determined using a slope method by plotting the experimental data in terms of ln(*MR*) vs. drying time and using equations (13) and (14):

$$\ln(MR) = -0.209981 - Bt \tag{13}$$

$$D_{eff} = \frac{-B}{\left(\frac{2.4674}{L^2}\right)} \tag{14}$$

Where D_{eff} is effective moisture diffusivity, $m^2 \cdot min^{-1}$; *B*, the slope of the linear equation. Eq. (14) was used to evaluate the effective moisture diffusivity of corn kernels under various drying temperatures.

The energy necessary for the removal of one molar moisture from a material of a given MC with similar composition is called as the activation energy [25]. According to Li et al. [26], the temperature dependence of effective moisture diffusivity can be provided by the Arrhenius association, as presented in eq. (15):

$$D_{eff} = D_0 \exp\left(-\frac{E_a}{RT}\right) \tag{15}$$

Where D_0 is the pre-exponential factor, E_a is the activation energy ($kJ \cdot mol^{-1}$), *R* is the universal gas constant (0.008314 $kJ \cdot mol^{-1} \cdot K^{-1}$), and *T* is absolute air temperature (K). The activation energy is determined from the slope of the plot, ln(D_{eff}) vs. $1/T$.

3. Results

3.1 *Changes in the temperature of grain layers and exhaust air during drying*

Figure 2 shows the alterations in temperature of each grain layer and exhaust air at various drying temperatures (45, 55, and 65 °C) and hot-air velocities (0.7, 1.1, and 1.3 $m \cdot s^{-1}$). At each drying temperature, at the initial grain layer (2.5 cm), the grain temperature quickly increased to a constant temperature and then showed a small fluctuation with drying time. Following an increase in drying temperature and hot-air velocity, the temperature lines were raised and shortened. The temperature lines in grain layers of 7.5 cm, 12.5 cm, 17.5 cm, 22.5 cm, and 27.5 cm all revealed saturation growth curves and took turns to lag. These lines were also raised and shortened with an increase in drying temperature and hot-air velocity. The temperature lines in the grain layer of 32.5 cm and in exhaust air demonstrated a quick increase with the first hour, and then increased slowly at 0.7 $m \cdot s^{-1}$ of hot air. Following an increase in hot air velocity from 0.7-1.3 $m \cdot s^{-1}$ and drying temperature from 45-65 °C, the temperature lines in the grain layer of 32.5 cm rose steadily. The temperature line in exhaust air showed a similar trend to that of the grain layer of 32.5 cm.

3.2 *Changes in interstitial air RH in grain layers and exhaust air during drying*

Figure 3 presents the alterations in interstitial airflow RH of each grain layer and exhaust air at various drying temperatures (45, 55, and 65 °C) and hot-air velocities (0.7, 1.1, and 1.3 $m \cdot s^{-1}$). For each drying temperature at the initial grain layer (2.5 cm), the interstitial airflow RH quickly decreased to the lowest value and remained unchanged with a lapsed drying time. Following an increase in drying temperature, the RH line at the same hot-air velocity

decreased to 0.1%. The interstitial airflow RH lines in grain layers of 7.5 cm, 12.5 cm, 17.5 cm, 22.5 cm, and 27.5 cm all had the shape of a hyperbolic line and took turns to lag, which show the contrary variation trends to temperature lines in grain layers in Figure 2. These RH lines were also raised and shortened with an increase in drying temperature and hot-air velocity. The interstitial airflow RH line in the grain layer of 32.5 cm at 0.7 $m \cdot s^{-1}$ hot-air velocity decreased slowly; however, it decreased quickly following increased hot-air velocity from 0.7-1.3 $m \cdot s^{-1}$. This line decreased quickly with an increase in drying temperature from 45-65 °C. The RH line in exhaust air demonstrated similar trends to that of a grain layer of 32.5 cm, both lines were also in contrast to temperature lines in grain layers in Figure 2.

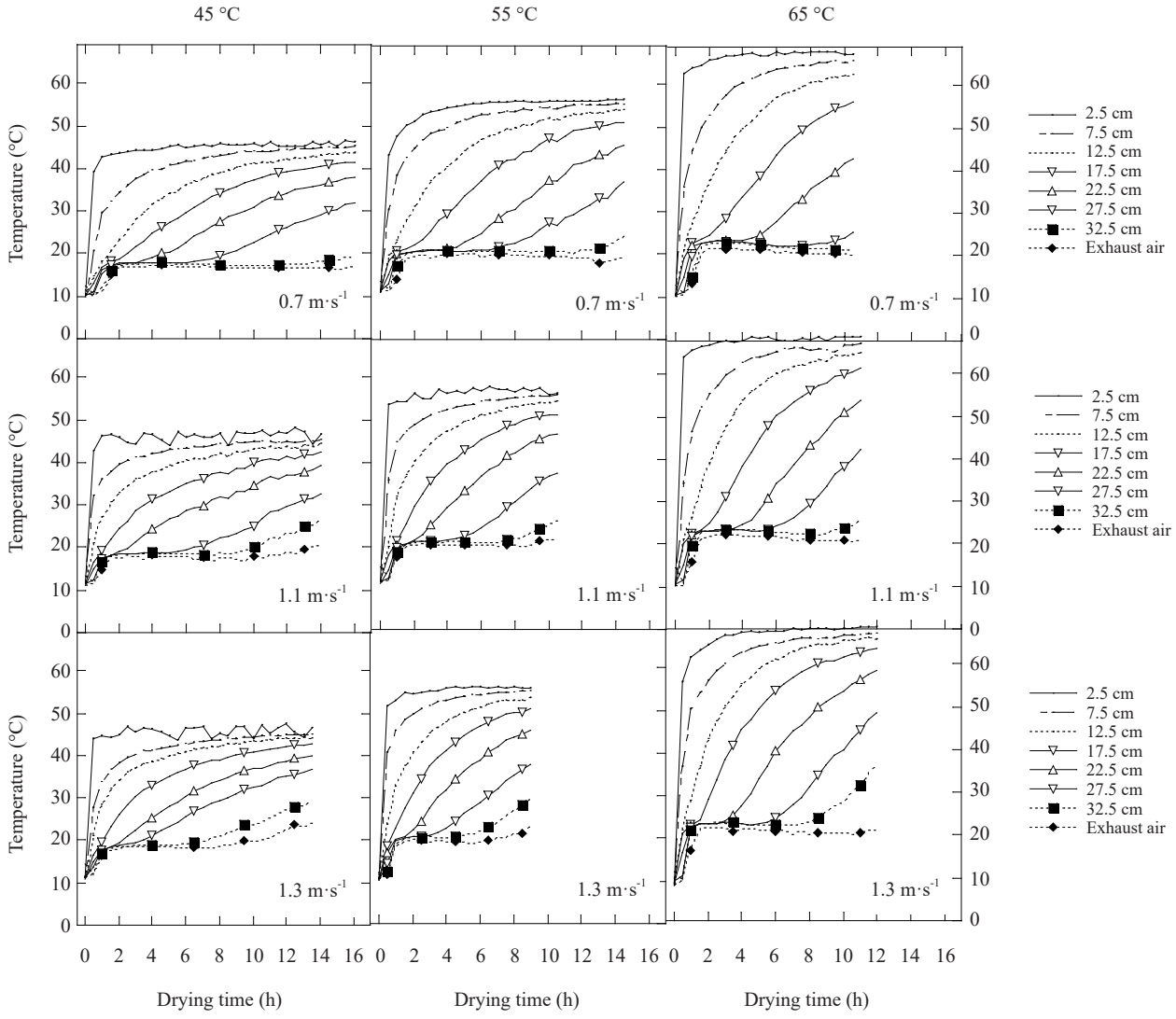

Figure 2. Changes in temperature of shelled corn grain layers and exhaust air

3.3 *Changes in sorption rates of shelled corn grain deep-layers during drying*

3.3.1 *Changes in moisture ratio (MR) with drying time at different airflow velocities*

Figures 4-6 show the changes in moisture ratio with drying time for drying shelled corn at 45, 55, 65 °C and hot-air velocities of 0.7, 1.1 and 1.3 $m \cdot s^{-1}$. The drying curves were plotted by the moisture ratio against the drying time. The drying time was reduced with an increase in the temperature of hot air because the rate of heat transfer increases with

drying temperature which could decrease the intergranular air RH and increase the transfer rate of moisture molecules from the kernels. As the drying time increased, the instantaneous moisture contents in the layers of 2.5 cm, 7.5 cm, and 12.5 cm rapidly decreased, but those in the layers of 17.5 cm, 22.5 cm, 27.5 cm, and 32.5 cm were relatively lagged to decrease. During the onset of the drying process, the drying rate was found to be high at the greatest moisture content but decreased as the moisture ratio declined. During the drying process, the water molecules present on the kernel surface firstly started getting removed and the surface could not keep in a saturated status because the rate of water transfer to the surface is not enough to remain saturated. This thus led to the decrease in drying rate as the kernel surface is not in an equilibrium status. After a rapid descent period of the drying rate and as the moisture level reached under the critical moisture content in the falling rate period, the drying rate continued to decrease until it reached the equilibrium moisture content (EMC). The higher interstitial airflow temperature and speed accelerated the decrease of MR in corn kernels.

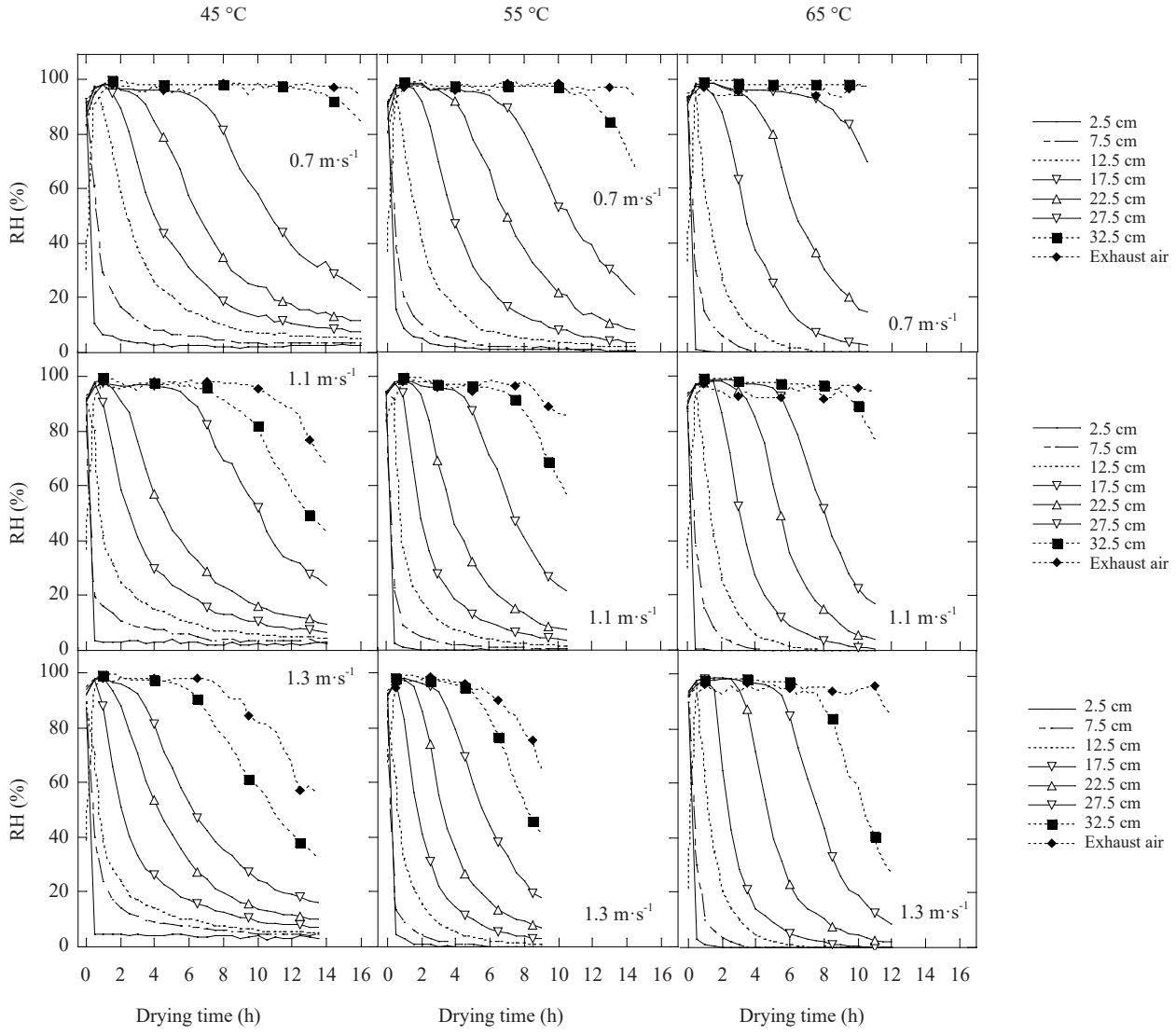

Figure 3. Changes in interstitial airflow relative humidity (RH) of shelled corn grain layers and exhaust air

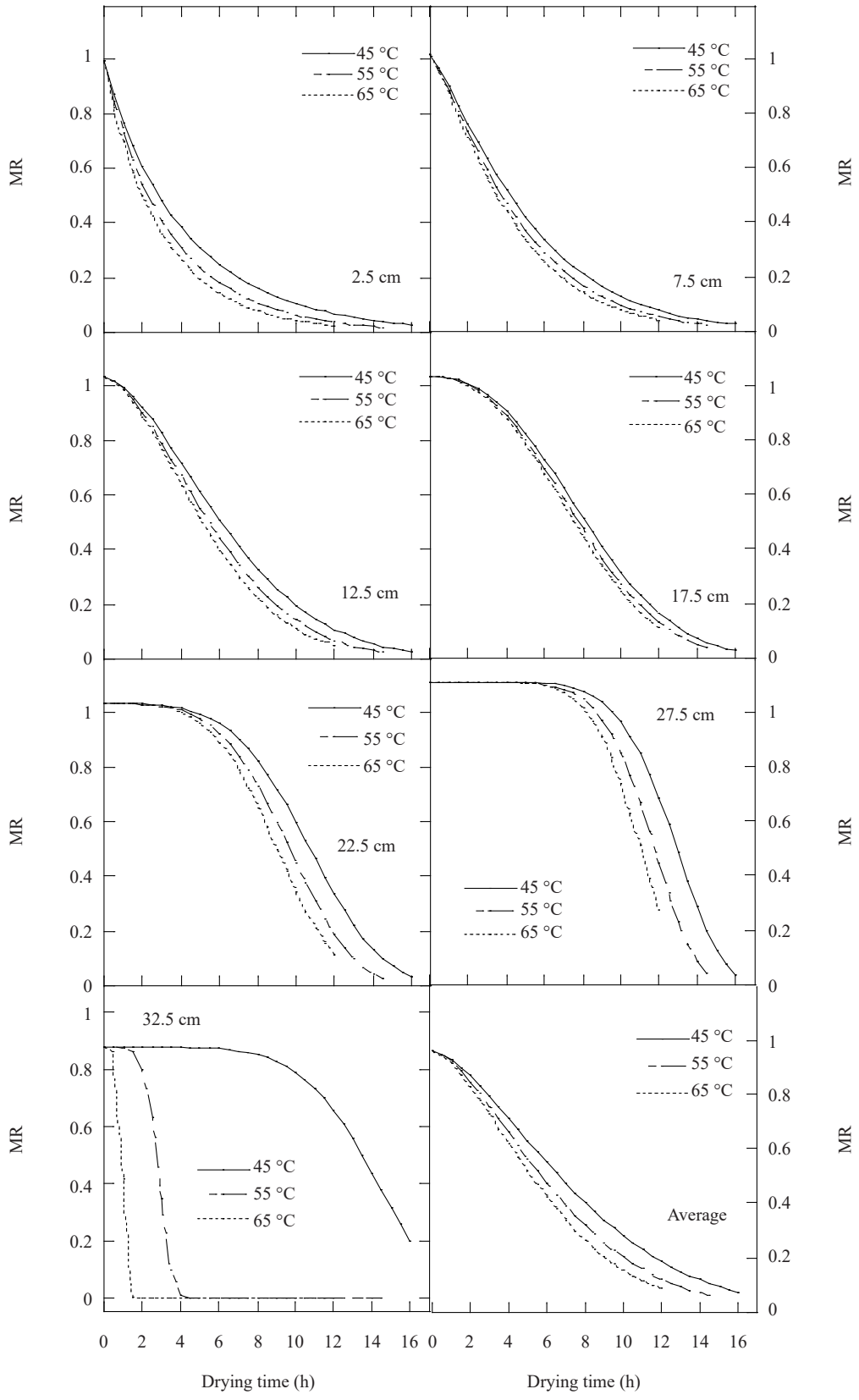

Figure 4. Changes in moisture ratio of shelled corn grain layers at hot-air velocity of 0.7 m/s

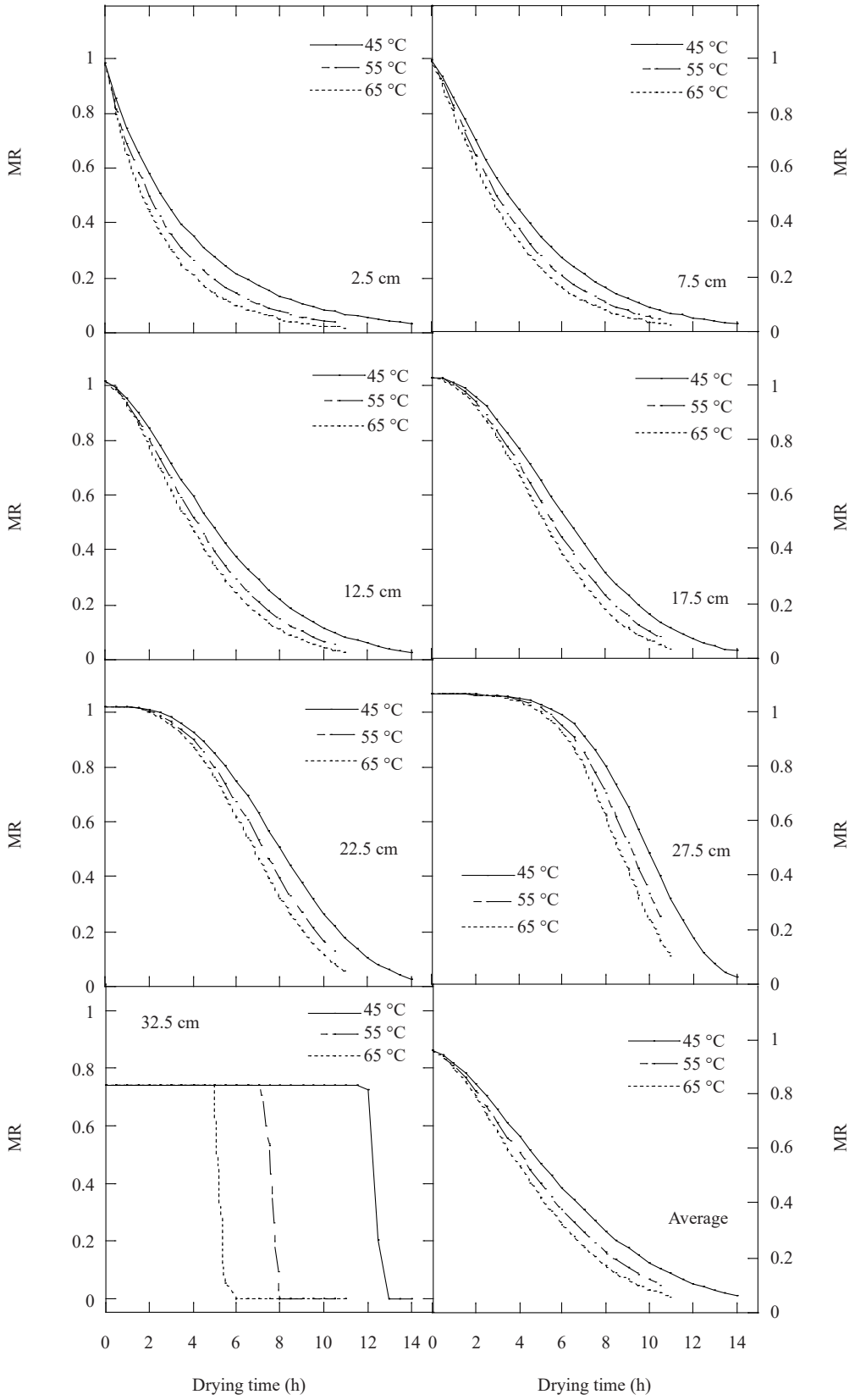

Figure 5. Changes in moisture ratio of shelled corn grain layers at a hot-air velocity of 1.1 m/s

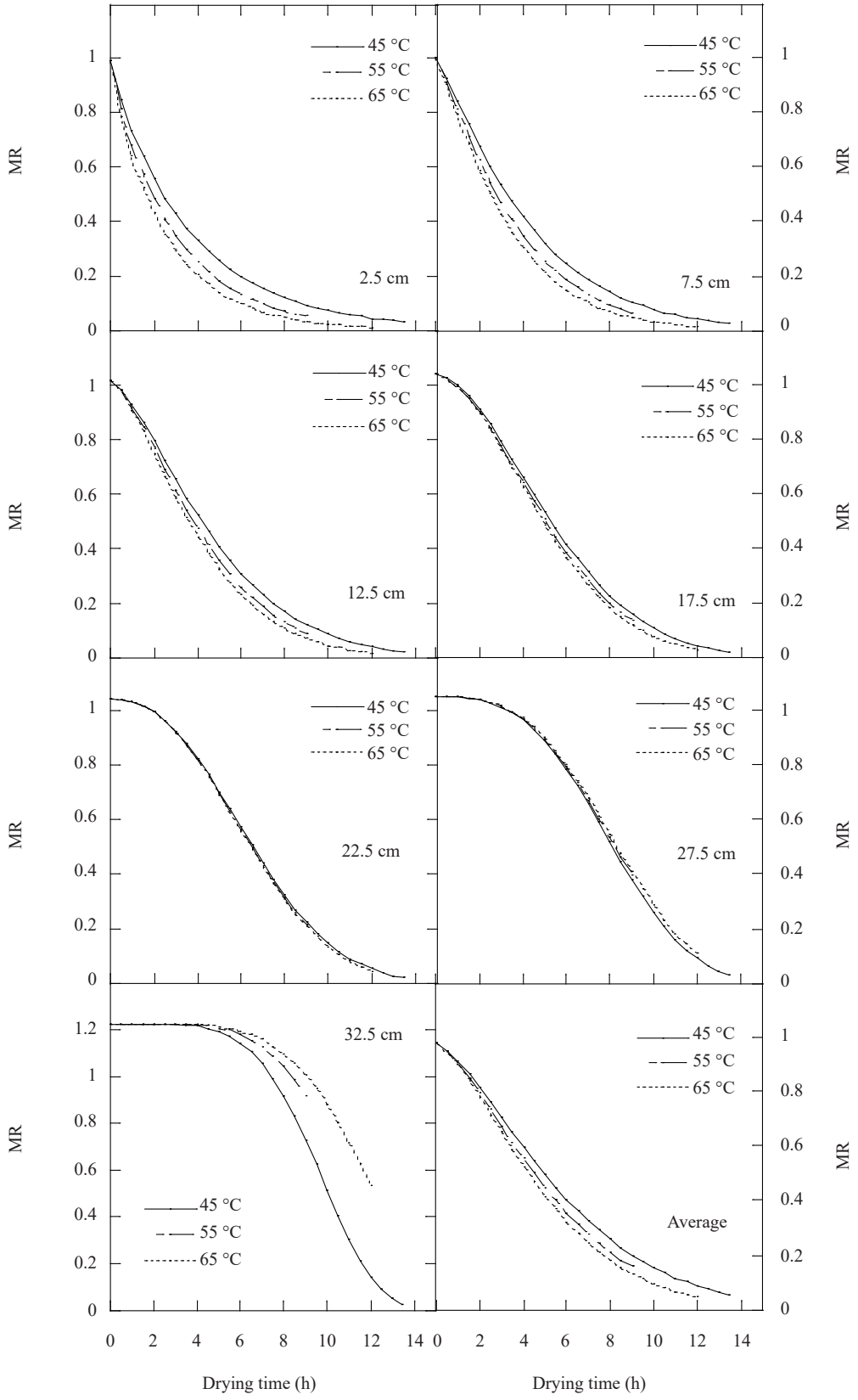

Figure 6. Changes in moisture ratio of shelled corn grain layers at a hot-air velocity of 1.3 m/s

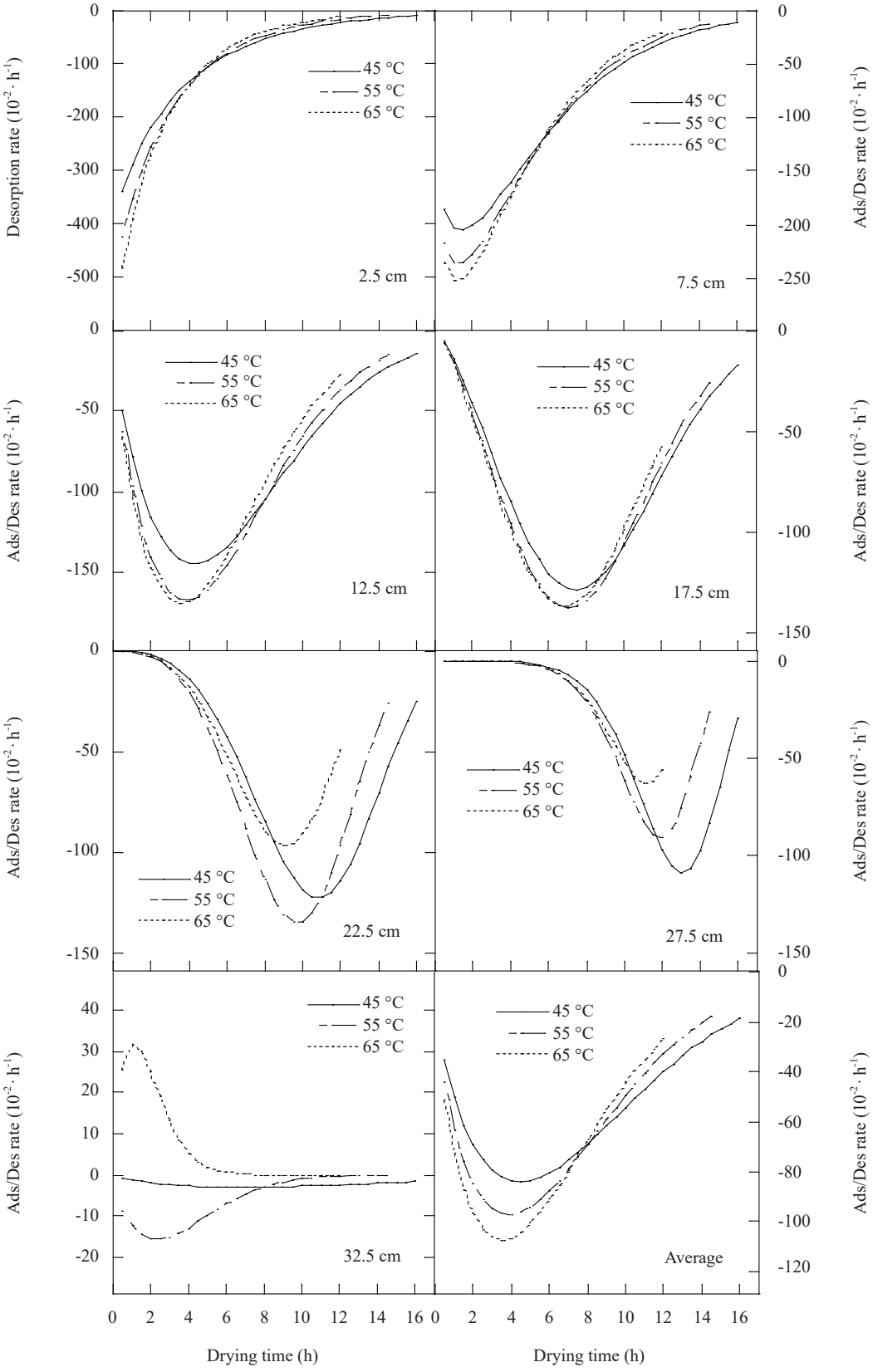

Note: Ads, adsorption; Des, desorption

Figure 7. Moisture sorption rates of the corn deep-layers at 0.7 m · s^{-1} of hot air

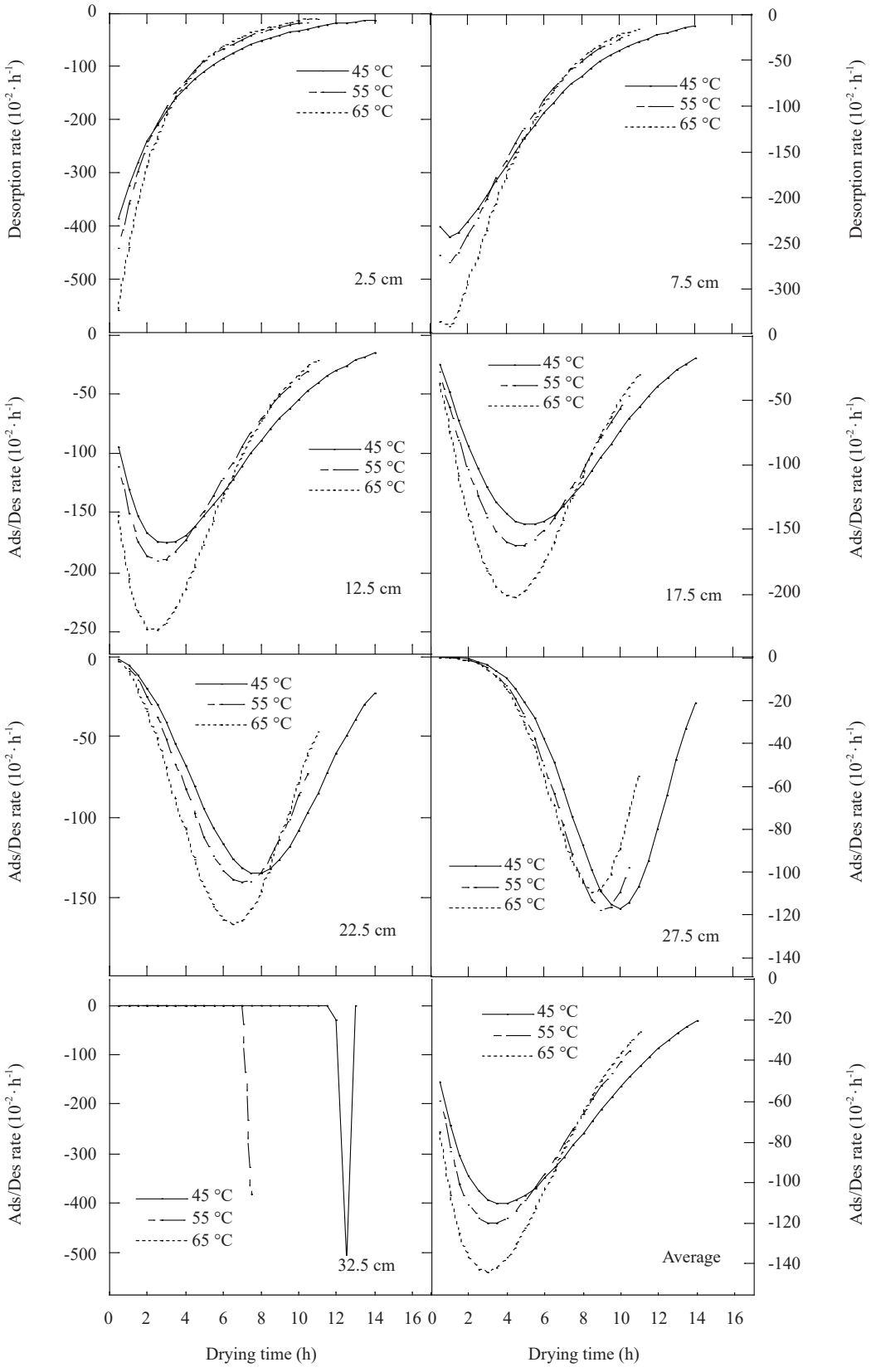

Figure 8. Moisture sorption rates of the shelled corn deep-layers at 1.1 m · s^{-1} of hot air

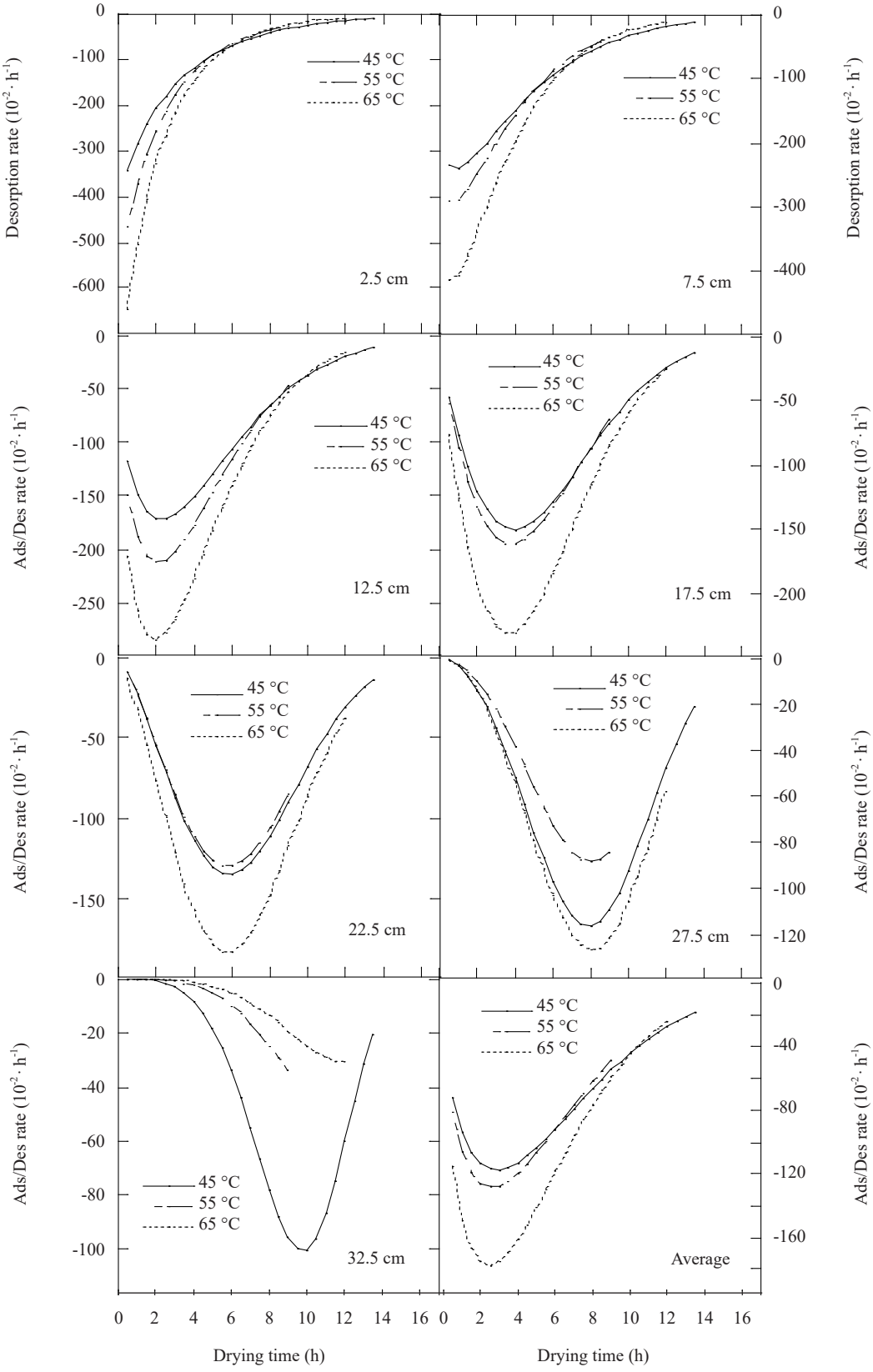

Figure 9. Moisture sorption rates of the corn deep-layers at 1.3 m · s^{-1} of hot air

3.3.2 *The fit of the modified diffusion equation to the plot of MR vs. time*

Table 1. Fitting of the modified diffusion equation (Eq. (3)) to the plot of MR versus time for the dried samples with different velocities of hot air

Hot-air velocity	Drying bed depth	Eq. (3) parameters				Statistical parameter			
		a	*k*	*n*	*b*	*RSS*	*SE*	R^2	*MRE*%
0.7 m·s^{-1}	2.5 cm	0.9916	7.00E-01	0.9469	40.3559	0.01404	1.67E-04	0.9977	1.0336
	7.5 cm	1.0151	2.37E-01	1.2275	26.1879	0.02763	3.29E-04	0.9966	1.4663
	12.5 cm	1.0278	8.54E-02	1.677	35.6898	0.07457	8.88E-04	0.9928	2.5167
	17.5 cm	1.0295	8.41E-03	2.4061	23.7002	0.06614	7.87E-04	0.9941	2.1423
	22.5 cm	1.0291	5.10E-04	3.9391	83.7746	0.24060	2.86E-03	0.9786	4.1584
	27.5 cm	1.1084	6.40E-07	6.7193	126.5885	1.17710	1.40E-02	0.8901	9.6080
	32.5 cm	0.9686	1.05E+02	1.6173	348.9968	23.8272	N.D.	N.D.	33.787
	Average[x]	0.9609	1.10E-01	1.5537	46.3776	0.10140	1.21E-03	0.9873	2.6156
1.1 m·s^{-1}	2.5 cm	0.9835	9.47E-01	0.9462	49.0615	0.02122	3.03E-04	0.9959	1.4055
	7.5 cm	0.9943	4.16E-01	1.1923	39.7932	0.02946	4.21E-04	0.9955	1.6808
	12.5 cm	1.0142	1.98E-01	1.5231	44.8304	0.05500	7.86E-04	0.9932	2.3363
	17.5 cm	1.0269	5.99E-03	2.0181	48.7819	0.12280	1.75E-03	0.9868	3.4570
	22.5 cm	1.0216	7.78E-03	2.8808	59.3183	0.26690	3.81E-03	0.9711	4.7266
	27.5 cm	1.0613	1.38E-04	4.5973	77.4645	0.80360	1.15E-02	0.9103	7.8001
	32.5 cm	0.7401	2.43E-02	97.9151	9,737.5454	58.8164	N.D.	N.D.	65.2922
	Average	0.9569	1.46E-01	1.5602	46.8817	0.09279	1.33E-03	0.9864	2.908
1.3 m·s^{-1}	2.5 cm	0.9841	9.10E-01	0.9356	44.6961	0.03388	4.98E-04	0.9934	1.796
	7.5 cm	0.9962	4.41E-01	1.1618	37.1621	0.05819	8.56E-04	0.9908	2.3789
	12.5 cm	1.0164	1.80E-01	1.4263	26.7688	0.1378	2.03E-03	0.9821	3.6215
	17.5 cm	1.0344	5.66E-02	1.7717	15.8021	0.2793	4.11E-03	0.9684	5.0019
	22.5 cm	1.0402	1.09E-02	2.3168	5.6513	0.5878	8.64E-03	0.9383	6.8151
	27.5 cm	1.0465	9.72E-04	3.0655	-8.3709	1.1355	1.67E-02	0.8754	8.6140
	32.5 cm	1.2291	1.03E-06	4.6951	-113.9709	6.4664	N.D.	N.D.	22.4967
	Average	0.9739	1.32E-01	1.4427	27.5953	0.2426	3.57E-03	0.9639	4.6581

Notes: *RSS*, residue sum of squares; *SE*, standard error; R^2, determination coefficient; *MRE*, mean relative percentage error. *a*, *k*, *n*, and *b* are parameters of eq. (3), *k* is the drying constant (h^{-1}). [x]average is the means of grain layer 2.5 to 32.5 cm. N.D., not detect

Table 1 presents the resulting fit of our modified diffusion equation (Eq. (3)) to the plot of MR vs. time for the corn samples during drying. With the exception of the grain layer of 32.5 cm, the other grain layers and average grain layers

revealed statistical parameters of $R^2 > 0.875$, $MRE < 9.61\%$, and less *RSS* and *SE*. This demonstrated that the coefficients of Eq. (3) can be used to analyze the moisture desorption rate of shelled corn kernels for 2.5-27.5 cm layers during drying. Furthermore, the 2.5-27.5 cm gain layers at three hot-air velocities show that parameter *n* in eq. (3) increased, whereas *k* decreased. For the grain layers of 2.5-32.5 cm, the average parameters *k* and *n* in eq. (3) at 1.1 $m \cdot s^{-1}$ hot-air velocity were highest among the three various hot-air velocities investigated.

3.3.3 *Moisture sorption rates of the corn deep-layers at various hot-air velocities*

Figure 7 presents the moisture sorption rates of the corn deep-layers from 2.5-32.5 cm at 0.7 $m \cdot s^{-1}$ hot air. The grain demonstrated decreased desorption rates with increased time in a parabolic manner, at a 2.5 cm grain layer for three drying temperatures from 45-65 °C. The grain desorption rate was lower at 45 °C than that at 65 °C. The 7.5 cm corn grain layer revealed adsorption at <1 h followed by desorption behavior, with a lower sorption rate at 45 °C than that at 65 °C. For the 12.5 cm, 17.5 cm, and 22.5 cm corn grain layers, the transition points from adsorption to desorption occurred at 3.5 h, 6.5 h, and 9.5 h with a drying temperature of 65 °C, respectively, and the grain initial sorption rates at 45 °C were significantly lower than that at 65 °C. The 27.5 cm corn grain layer demonstrated an unchanged during the initial 4 h followed by adsorption, and the transition points to desorption were at 8 h, 9.8 h, and 11 h for 65 °C, 55 °C, and 45 °C drying temperatures, respectively. For the 32.5 cm corn grain layer, the grain revealed desorption at 65 °C during the first 1 h followed by adsorbed moisture from 1-5 h. Adsorption of the grain at 55 °C drying was observed during the first 2 h, followed by desorbed moisture at 2-10 h; however, the grain at 45 °C drying demonstrated a slow adsorption rate throughout the entire duration of drying. The overall grain layers of 2.5-32.5 cm revealed initial desorption rates that gradually decreased for the three drying temperatures. The transition points from adsorption to desorption occurred at 3.5 h, 4.0 h, and 4.5 h at 65 °C to 45 °C drying temperatures, as revealed by the average sorption rate curve for 2.5-32.5 cm grain layers (Figure 7).

Figure 8 presents the moisture sorption rates of the corn deep-layers from 2.5-32.5 cm at 1.1 $m \cdot s^{-1}$ hot air. At a 2.5 cm corn grain layer, for three drying temperatures of 45-65 °C, the grains demonstrated desorption and the initial desorption rates were higher than those dried at 0.7 $m \cdot s^{-1}$ of hot air. The lag effect in grain desorption rate between 45 °C and 65 °C at 1.1 $m \cdot s^{-1}$ of hot air was larger than that at 0.7 $m \cdot s^{-1}$ hot air. For the 7.5 cm corn grain layer, the grain revealed adsorption during the first 1 h, followed by desorption behavior, and the higher initial desorption rate for 65-45 °C occurred at 1.1 $m \cdot s^{-1}$ hot air rather than at 0.7 $m \cdot s^{-1}$ hot air. For 12.5 cm, 17.5 cm, and 22.5 cm corn grain layers, the transition points from adsorption to desorption occurred at 3.2 h, 4.3 h, and 6.5 h for a drying temperature of 65 °C, respectively; the grain initial sorption rate at 45°C was significantly lower than at 65 °C. For the 27.5 cm corn grain layer, the sorption rate remained unchanged during the first 2 h followed by adsorption, and the transition points to desorption were at 8.5 h, 9.0 h, and 10 h for 65 °C, 55 °C, and 45 °C drying temperatures, respectively. For the 32.5 cm corn grain layer, the grains at 55 °C and 45 °C drying demonstrated a brief adsorption transition to desorption at 7.5 h and 12.5 h, respectively. For the overall grain layers of 2.5-27.5 cm, the initial desorption rates at 1.1 $m \cdot s^{-1}$ of hot air gradually decreased for three drying temperatures, but were higher than the corresponding rates at 0.7 $m \cdot s^{-1}$ hot air. For the average sorption rate curve of the grain layers of 2.5-32.5 cm at 1.1 $m \cdot s^{-1}$ hot air, the transition points from adsorption to desorption occurred at 2.8 h, 3.2 h, and 3.8 h for the drying temperatures of 65-45 °C, respectively, and revealed earlier and higher initial desorption rates compared with those at 0.7 $m \cdot s^{-1}$ hot air.

Figure 9 presents moisture sorption rates of the corn deep-layers from 2.5-32.5 cm at 1.3 $m \cdot s^{-1}$ hot air. For the 2.5 cm corn grain layer at three drying temperatures from 45-65 °C, the grains only demonstrated desorption, and the initial desorption rates were higher than those dried at 1.1 $m \cdot s^{-1}$ hot air. The lag effect in grain initial desorption rate between 45 and 65 °C at 1.3 $m \cdot s^{-1}$ of hot air was larger than that of 1.1 $m \cdot s^{-1}$ hot air. For the 7.5 cm corn grain layer, the grain revealed brief adsorption in the first 0.5-1 h followed by desorption behavior, and the higher desorption rate for 65-45 °C occurred at 1.3 $m \cdot s^{-1}$ hot air than that at 1.1 $m \cdot s^{-1}$ hot air. For the 12.5 cm, 17.5 cm, and 22.5 cm corn grain layers, the transition points from adsorption to desorption occurred at 2.8 h, 3.8 h, and 5.8 h for a drying temperature of 65 °C, respectively; the grain initial desorption rate at 45 °C was significantly slower than that at 65 °C. For the 27.5 cm corn grain layer, the grain quickly demonstrated adsorption and the transition points to desorption were at 8.2 h, 7.8 h, and 7.8 h for 65 °C, 55 °C, and 45 °C drying temperatures, respectively. For the 32.5 cm corn grain layer, the grain at 65 °C and 55 °C drying temperatures revealed adsorption from 2.0-11.5/-9.0 h, respectively; however, the grain at 45 °C drying temperature transitioned from adsorption to desorption at 9.8 h. For the whole grain layers of 2.5-27.5 cm,

the initial desorption rates at 1.3 $m \cdot s^{-1}$ hot air gradually decreased for three drying temperatures, but were higher than the corresponding rates at 1.1 $m \cdot s^{-1}$ hot air. For the average sorption rate curve for the grain layers of 2.5-32.5 cm at 1.3 $m \cdot s^{-1}$ of hot air, the transition points from adsorption to desorption occurred at 2.4 h, 2.7 h, and 3.0 h for the drying temperatures of 65-45 °C, respectively, and represented earlier and larger initial desorption rates than those at 1.1 $m \cdot s^{-1}$ hot air.

Table 2. Effective diffusion coefficient of corn kernels at different drying temperatures and hot-air velocity

Drying bed depth (cm)	Drying temp. (°C)	Effective diffusion coefficient ($m^2 \cdot h^{-1}$)		
		0.7 $m \cdot s^{-1}$	1.1 $m \cdot s^{-1}$	1.3 $m \cdot s^{-1}$
2.5	45	8.728E-07	8.276E-07	7.805E-07
7.5	45	7.951E-07	9.085E-07	1.071E-06
12.5	45	8.428E-07	1.002E-06	9.354E-07
17.5	45	5.703E-07	7.073E-07	9.970E-07
22.5	45	6.967E-07	5.093E-07	8.603E-07
27.5	45	2.917E-07	3.773E-07	7.361E-07
32.5	45	9.343E-08	2.212E-07	6.285E-07
2.5	55	8.301E-07	1.406E-06	1.719E-06
7.5	55	7.397E-07	1.429E-06	1.182E-06
12.5	55	8.434E-07	1.300E-06	1.667E-06
17.5	55	5.930E-07	1.262E-06	1.479E-06
22.5	55	6.782E-07	1.113E-06	8.603E-07
27.5	55	2.193E-07	8.963E-07	1.115E-06
32.5	55	2.811E-06	6.072E-07	2.714E-07
2.5	65	1.191E-06	1.431E-06	1.398E-06
7.5	65	1.101E-06	1.387E-06	1.327E-06
12.5	65	8.534E-07	1.243E-06	1.284E-06
17.5	65	5.404E-07	8.345E-07	1.124E-06
22.5	65	5.082E-07	6.019E-07	9.695E-07
27.5	65	2.423E-07	3.324E-07	4.375E-07
32.5	65	1.520E-06	3.085E-06	6.876E-08
Average	45	5.478E-07	6.144E-07	8.315E-07
Average	55	7.807E-07	7.738E-07	1.423E-06
Average	65	6.879E-07	7.355E-07	7.186E-07

Note: Average is the means of grain layer 2.5 to 32.5 cm

Table 3. Effective activation energy of corn kernels at different hot-air velocity

Hot-air velocity	Drying bed depth (cm)	Temp. range (°C)	D_0 ($m^2 \cdot h^{-1}$)	Activation energy ($KJ \cdot mol^{-1}$)
	2.5	45-65	1.333E-04	13.26
	7.5	45-65	1.528E-04	13.88
	12.5	45-65	1.033E-06	0.53
0.7 $m \cdot s^{-1}$	17.5	45-65	2.429E-07	-2.28
	22.5	45-65	3.988E-09	-13.55
	27.5	45-65	1.174E-08	-8.20
	32.5	45-65	5.120E+13	122.61
	2.5	45-65	8.941E-03	23.96
	7.5	45-65	1.211E-03	18.53
	12.5	45-65	4.005E-05	9.47
1.1 $m \cdot s^{-1}$	17.5	45-65	1.545E-05	7.61
	22.5	45-65	1.307E-05	7.86
	27.5	45-65	8.504E-08	-4.66
	32.5	45-65	1.988E+12	113.86
	2.5	45-65	1.766E-02	25.68
	7.5	45-65	3.764E-05	9.27
	12.5	45-65	2.411E-04	14.10
1.3 $m \cdot s^{-1}$	17.5	45-65	9.121E-06	5.48
	22.5	45-65	6.042E-06	5.12
	27.5	45-65	2.007E-10	-21.93
	32.5	45-65	7.670E-23	-95.61
0.7 $m \cdot s^{-1}$	Average	45-65	2.837E-05	10.07
1.1 $m \cdot s^{-1}$	Average	45-65	1.349E-05	7.92
1.3 $m \cdot s^{-1}$	Average	45-65	1.103E-07	-5.77

Note: Average is the means of grain layer 2.5 to 32.5 cm

3.4 *Changes in effective moisture diffusivity and activation energy of grain deep-layers during drying*

Table 2 presents the effective diffusion coefficients of corn kernels at various drying temperatures and hot-air velocities. For drying temperatures of 45 °C at 0.7 $m \cdot s^{-1}$ hot-air velocity, the effective diffusion coefficient (D_{eff}) of corn kernels decreased with an increase in drying bed depth from 2.5 to 32.5 cm; however, at 1.1 $m \cdot s^{-1}$ hot-air velocity, the D_{eff} values increased to 1.002×10^{-6} $m^2 \cdot h^{-1}$ from 2.5 to 12.5 cm bed depths, and thereafter decreased with an increase

in bed depth. At 1.3 $m \cdot s^{-1}$ hot-air velocity, the D_{eff} values increased to 1.071×10^{-6} $m^2 \cdot h^{-1}$ at a bed depth of 7.5 cm, and thereafter continuously decreased with an increase in bed depth.

For the drying temperature of 55 °C at 1.1 $m \cdot s^{-1}$ hot-air velocity, the D_{eff} values of corn kernels decreased with an increase in drying bed depth from 2.5 to 32.5 cm. For the 0.7 and 1.3 $m \cdot s^{-1}$ hot-air velocities, with the exception of 2.811×10^{-6} $m^2 \cdot h^{-1}$ at 32.5 cm and 1.115×10^{-6} $m^2 \cdot h^{-1}$ at 27.5 cm, respectively, the D_{eff} values decreased with an increase in bed depth.

For a drying temperature of 65 °C at 1.3 $m \cdot s^{-1}$ hot-air velocity, the D_{eff} values of corn kernels decreased with an increase in drying bed depth from 2.5 to 32.5 cm. For 0.7 and 1.1 $m \cdot s^{-1}$ hot-air velocities, with the exception of 1.520×10^{-6} $m^2 \cdot h^{-1}$ and 3.085×10^{-6} $m^2 \cdot h^{-1}$ at 32.5 cm, respectively, the D_{eff} values decreased with an increase in bed depth.

Compared with the average value from grain layers, at the same hot-air velocity, the D_{eff} values of corn kernels dried at 55 °C were correspondingly greater than those dried at 45 °C and 65 °C. At the same drying temperature, the D_{eff} values of corn kernels increased with an increase in hot-air velocity.

Table 3 presents the effective activation energy of corn kernels at various hot-air velocities. For 0.7 and 1.1 $m \cdot s^{-1}$ hot-air velocity, with the exception of values at 32.5 cm bed depth due to a boundary effect, the pre-exponential factor of Arrhenius equation (D_0) and activation energy decreased with an increase in bed depth. For the 1.3 $m \cdot s^{-1}$ hot-air velocity, the D_0 and activation energy decreased with an increase in bed depth.

Compared with the average value from grain layers, at the same drying temperature range of 45-65 °C, the D_0 and activation energy values of corn kernels decreased with an increase in hot-air velocity from 0.7 to 1.3 $m \cdot s^{-1}$. This study investigated the drying kinetics, and effective moisture diffusivities of Chinese shelled corn in low-temperature deep-bed drying devices, including developing mathematical models for predicting free moisture content, drying curves, and effective moisture diffusivities. The changes in the characteristic constituents of shelled corn during drying should be studied by nuclear magnetic resonance spectroscopy (NMRS).

4. Discussion

The adsorption and desorption method was most commonly used to collect data for the determination of the diffusion coefficient in grain, compared with the permeation method, concentration-distance curves method, radio tracer method, and nuclear magnetic resonance and self-diffusion method [27]. The differences in the diffusion coefficients developed from the various models available are substantial. Assuming a yellow-dent corn kernel with a brick shape, Pabis and Henderson [28] revealed that at a drying air temperature of approximately 38 °C and an initial MC (IMC) of 23%, the moisture diffusion coefficient was approximately 1.302×10^{-7} $m^2 \cdot h^{-1}$. Chittenden and Hustrulid [29] demonstrated that, for the same temperature, the moisture diffusion coefficient was determined to be 4.021×10^{-8} $m^2 \cdot h^{-1}$ for sphere kernel-shaped corn. In the present study, the Chinese corn kernel was assumed as a homogenous infinite slab, and the effective diffusion coefficients at a 45 °C drying temperature were; 5.478×10^{-7}, 6.144×10^{-7}, and 8.315×10^{-7} $m^2 \cdot h^{-1}$ with a hot-air velocity of 0.7, 1.1, and 1.3 $m \cdot s^{-1}$, respectively. These results were similar to those revealed in a previous study by Muthukumarappan and Gunasekaran [30] with infinite slab kernel geometry, which evaluated the reported vapor diffusivity values for two corn varieties, K6400 (1.524×10^{-7}-4.318×10^{-7} $m^2 \cdot h^{-1}$) and Dekalb 547 (1.502×10^{-7}-4.087×10^{-7} $m^2 \cdot h^{-1}$), at 40 °C and RH 75-95%. The results of the present study indicated that our modified Page's model (eq. (3)) was an effective fitting model for drying at 45-65 °C.

Graphical and least squares techniques are usually used to analyze adsorption and desorption rates when determining the moisture diffusion coefficient. A number of models have been proposed to describe the rate of moisture loss during thin-layer drying of biological materials [7, 31]. The majority of previous studies plotted *MR* against the time of exposure for each sample, describing the moisture absorbed or desorbed at a given time. In thin-layer drying experiments, the *MR* always decreased with elapsed drying time in a parabolic form [32]. However, in the simulation of deep bed drying, the adsorptive behavior is difficult to reveal by plotting the experimental data in terms of *MR* vs. drying time. The present study developed Eq. (3) and adopted $d(M_t)/dt$ to evaluate the change in desorption rate of shelled corn, and demonstrated that corn kernels first underwent adsorption, followed by desorption, with an increased drying bed depth from 7.5-32.5 cm.

The *k* value in the modified form of Page's equation primarily identified the rate of moisture transport [25, 33].

For 2.5-27.5 cm gain layers at three hot-air velocities, the parameter k in eq. (3) decreased with grain bed depth, and the desorption rate as described by the $d(M_t)/dt$ also had a trend to decrease. Following an increase in drying temperature and hot-air velocity, the adsorption time decreased and the desorption rate in each layer increased. All three factors: drying temperature, hot-air velocity, and grain layer position, had a great effect on the rate of adsorption or desorption. These findings indicated that the higher drying temperature and hot-air velocity induced the increased effective moisture diffusivity and desorption rate.

In the present study, at 0.7-1.3 $m \cdot s^{-1}$ hot-air velocity, for the whole bed depth, the average activation energy of shelled corn was -5.77-10.03 $kJ \cdot mol^{-1}$, smaller than the value (29.56 $kJ \cdot mol^{-1}$) obtained for corn thin-layer drying reported by Doymaz and Pala [34]. At the 2.5 cm drying layer, the activation energy ranged from 13.26-25.68 $kJ \cdot mol^{-1}$ for the three hot-air velocities investigated. At the same hot-air velocity, the D_{eff} values of corn kernels dried at 55 °C were correspondingly larger than those dried at 45 °C and 65 °C. At the same drying temperature, the D_{eff} values of corn kernels tended to increase with an increase in hot-air velocity, whereas the activation energy was observed to decrease. These results suggested that increasing drying-air temperature and airflow velocity may shorten adsorption time and increase desorption rate in deep-bed drying, thus increasing the drying capacity and reducing drying time. Further investigation is required to gain more knowledge of the association between the physical and chemical compositions of shelled corn and their possible effects on the wetting or drying rates, and to determine the optimum combinations of the operating parameters (i.e., bed depth, reversal MC, airflow rate, and drying air temperatures).

5. Conclusion

The interstitial airflow RH lines in grain layers of 7.5-27.5 cm in a low-temperature deep-bed drying column device had the shape of a hyperbolic line and took turns to lag. These RH lines and temperature lines were shortened with an increase in drying temperature and hot-air velocity. As the drying time increased, the instantaneous moisture contents in the layers of 2.5 cm, 7.5 cm, and 12.5 cm rapidly decreased, but those in the layers of 17.5 cm, 22.5 cm, 27.5 cm and 32.5 cm were relatively lagged to decrease. The coefficients of our modified Eq. (3) can be used to analyze the moisture desorption rate of corn kernels from 2.5-27.5 cm layers during drying. For the average sorption rate curve from grain layers of 2.5-32.5 cm at 1.3 $m \cdot s^{-1}$ of hot air, the transition points from adsorption to desorption occurred at 2.4 h, 2.7 h, and 3.0 h for the drying temperatures of 65-45 °C, respectively, and were earlier and larger compared with those at 1.1 $m \cdot s^{-1}$ of hot air. Compared with the average value from grain layers, at the same hot-air velocity, the D_{eff} values of corn kernels dried at 55 °C were correspondingly larger than those dried at 45 °C and 65 °C. At the same drying temperature, the D_{eff} values of corn kernels tended to increase with an increase in hot-air velocity. At the same hot-air velocity, the D_0 and activation energy values of corn kernels dried at temperatures of 45-65 °C tended to decrease with an increase in grain bed depth. At the same drying temperature range, the D_0 and activation energy values of corn kernels tended to decrease with an increase in hot-air velocity. This study can help to optimize the drying processes of high moisture shelled corn.

Acknowledgments

The authors would like to acknowledge the Special Fund for Grain Scientific Research in the Public Interest from the State Administration of Grains, China (201313001-03-01).

Conflict of interest

The authors declare that there are no conflicts of interest regarding the publication of this article.

References

[1] Jiang P, Li XJ. Effective moisture diffusivity and thermal property of shelled corn during drying (In Chinese with English Abstract). *Science and Technology of Food Industry*. 2016; 37(15): 53-58. Available from: doi: 10.13386/j.issn1002-0306.2016.15.002.

[2] Wei Z, Yusan YS, Li XJ, Zhao MH, Wu JZ, Yan EF. Changes in intergranular air properties and chemical parameters of short-term stored bulk shelled corn with slightly high moisture content. *Modern Agriculture and Biotechnology*. 2023; 2(4): 22. Available from: doi: 10.53964/jmab.2023022.

[3] Abdoli B, Zare D, Jafari A, Chen GN. Evaluation of the air-borne ultrasound on fluidized bed drying of shelled corn: Effectiveness, grain quality, and energy consumption. *Drying Technology*. 2018; 36(14): 1749-1766. Available from: doi: 10.1080/07373937.2018.1423568.

[4] Amantea RP, Sarri D, Rossi G. A system dynamic modeling to evaluate fluidized bed dryers under tempering and recirculation strategies. *Applied Chemical Engineering*. 2024; 7(1): 1-8. Available from: doi: 10.24294/ace.v7i1.3276.

[5] Okunola AA, Adekanye TA, Okonkwo CE, Kaveh M, Szymanek M, Idahosa EO, et al. Drying characteristics, kinetic modeling, energy and exergy analyses of water yam (*Dioscorea alata*) in a hot air dryer. *Energies*. 2023; 16: 1569. Available from: doi: 10.3390/en16041569.

[6] Jamil Z, Mohite AM, Sharma N. Selected engineering properties and drying behavior of tendu (*Diospyros melanoxylon roxb*.) fruit. *Current Research in Nutrition and Food Science*. 2020; 8(2): 622-629. Available from: doi: 10.12944/CRNFSJ.8.2.27.

[7] Jha AK, Sit N. Drying characteristics and kinetics of colour change and degradation of phytocomponents and antioxidant activity during convective drying of deseeded Terminalia chebula fruit. *Journal of Food Measurement and Characterization*. 2020; 14(3): 2067-2077. Available from: doi: 10.1007/s11694-020-00454-9.

[8] Sootjarit S, Jittanit W, Phompan S, Rerkdamri P. Moisture sorption behaviour and drying kinetics of pre-germinated rough rice and pre-germinated brown rice. *Transactions of the ASABE*. 2011; 54(1): 255-263.

[9] Myhan R, Markowski M. Generalized mathematical model of the grain drying process. *Prcoesses*. 2022; 10: 2749. Available from: doi: 10.3390/pr10122749.

[10] Midilli A, Kucuk H, Yapar Z. A new model for single-layer drying. *Drying Technology*. 2002; 20(7): 1503-1513. Available from: doi: 10.1081/drt-120005864.

[11] Müller A, Nunes MT, Maldaner V, Coradi PC, de Moraes RS, Martens S, et al. Rice drying, storage and processing: effects of post-harvest operations on grain quality. *Rice Science*. 2022; 29(1): 16-30. Available from: doi: 10.1016/j.rsci.2021.12.002.

[12] ASAE. S448 DEC93. *Thin-Layer Drying of Grains and Crops*. St. Joseph, Mich: ASAE; 1994. p. 482-484.

[13] Li XJ. *The Theory and Practice of Grain Equilibrium Moisture*. Beijing, China: China Light Industry Press; 2022. p. 202-204.

[14] Panigrahi SS, Singh CB, Fielke J. A 3D transient CFD model to predict heat and moisture transfer in on-farm stored grain silo through parallel computing using compiler directives: Impact of discretization methods on solution efficacy. *Drying Technology*. 2022; 41(7): 1133-1147. Available from: doi: 10.1080/07373937.2022.2121284.

[15] Walton LR, Casada ME. A new diffusion model for drying Burley tobacco. *Transaction of the ASAE*. 1986; 29(1): 271-275. Available from: doi: 10.13031/2013.30138.

[16] Walton LR, White GM, Ross IJ. A cellular diffusion-based drying model for corn. *Transaction of the ASAE*. 1988; 31(1): 279-283. Available from: doi: 10.13031/2013.30700.

[17] Kashaninejad M, Mortazavi A, Safekordi A, Tabil LG. Thin-layer drying characteristics and modeling of pistachio nuts. *Journal of Food Engineering*. 2007; 78(1): 98-108. Available from: doi: 10.1016/j.jfoodeng.2005.09.007.

[18] Jittanit W, Srzednicki G, Driscoll R. Seed drying in fluidized and spouted bed dryers. *Drying Technology*. 2010; 28(10): 1213-1219. Available from: doi: 10.1080/07373937.2010.483048.

[19] Tabatabaee R, Jayas DS, White NDG. Thin-layer drying and rewetting characteristics of buckwheat. *Canadian Biosystems Engineering*. 2003; 46(3): 19-24.

[20] China National Standard. GB/T 5497-85. *Inspection of grain and oilseeds - Methods for determination of moisture content*. Standardization Administration of the People's Republic of China; 1986.

[21] Synergy Software. *Kaleidagraph for Windows version 4.54 software*. Pennsylvania, USA: Synergy; 2021.

[22] SPSS Inc. *SPSS for Windows, Release 18.0.1*. Chicago, USA: SPSS Inc.; 2017.

[23] Li XJ, Han X, Tao LS, Jiang P, Qin W. Sorption equilibrium moisture and isosteric heat of Chinese wheat bran products added to rice to increase its dietary fiber content. *Grain & Oil Science and Technology*. 2021; 4: 149-161.

Available from: doi: 10.1016/j.gaost.2021.09.001.
[24] Tulek Y. Drying kinetics of oyster mushroom (*Pleurotus ostreatus*) in a convective hot air dryer. *Journal of Agricultural Science and Technology*. 2011; 13: 655-664.
[25] Fang S, Wang Z, Hu X. Hot air drying of whole fruit Chinese jujube (*Zizyphus jujuba Miller*): thin-layer mathematical modelling. *International Journal of Food Science & Technology*. 2009; 44(9): 1818-1824. Available from: doi: 10.1111/j.1365-2621.2009.02005.x.
[26] Li XJ, Wang X, Li Y, Jiang P, Lu H. Changes in moisture effective diffusivity and glass transition temperature of paddy during drying. *Computers and Electronics in Agriculture*. 2016; 128: 112-119. Available from: doi: 10.1016/j.compag.2016.08.025.
[27] Yu X, Schmidt AR, Bello-Perez LA, Schmidt SJ. Determination of the bulk moisture diffusion coefficient for corn starch using an automated water sorption instrument. *Journal of Agricultural and Food Chemistry*. 2008; 56: 50-58. Available from: doi: 10.1021/jf071894a.
[28] Pabis S, Henderson HM. Grain drying theory, II. A critical anaylsis of the drying curve for shelled maize. *Journal of Agricultural Engineering Research*. 1961; 6(4): 272-277.
[29] Chittenden DH, Hustrulid A. Determining drying constants for shelled corn. *Transaction of the ASAE*. 1966; 9(1): 52-55. Available from: doi: 10.13031/2013.39872.
[30] Muthukumarappan K, Gunasekaran S. Vapor diffusivity and hygroscopic expansion of corn kernels during adsorption. *Transaction of the ASAE*. 1990; 33(5): 1637-1641.
[31] Mohapatra D, Rao PS. A thin-layer drying model of parboiled wheat. *Journal of Food Engineering*. 2005; 66(4): 513-518. Available from: doi: 10.1016/j.jfoodeng.2004.04.023.
[32] ANSI/ASAE. S448.2. *Thin-Layer Drying of Agricultural Crops*. St. Joseph, Mich: ASABE; 2014.
[33] McNeill SG, Henry ZA, Wilhelm LR, Walton LR. Delayed harvest effects on moisture sorption properties of soybeans. *Applied Engineering in Agriculture*. 2001; 17(3): 329-340. Available from: doi: 10.13031/2013.6200.
[34] Doymaz I, Pala M. The thin-layer drying characteristics of corn. *Journal of Food Engineering*. 2003; 60(2): 125-130. Available from: doi: 10.1016/s0260-8774(03)00025-6.